

## Velocity interferometry technique used to measure the expansion and compression phases of a sonoluminescent bubble

Gerardo A. Delgadino and Fabian J. Bonetto

*Department of Environmental and Energy Engineering and Center for Multiphase Research, Rensselaer Polytechnic Institute, Troy, New York 12180-3590*

(Received 23 July 1997)

We ultrasonically levitated single bubbles of about ten micrometers in diameter and focused two laser beams on them. We recorded a photodetector voltage as a function of time in a storage oscilloscope. Doppler shift in the scattered light produces intensity oscillations. We used these oscillations to obtain the rate of compression and expansion of the bubble. The maximum measured compression velocity was estimated to be 350 m/s with an uncertainty of 20%. [S1063-651X(97)50812-9]

PACS number(s): 78.60.Mq

Sonoluminescence was discovered in 1933 by Marinenco and Trillat [1]. In this phenomenon, acoustical energy is concentrated by an oscillating bubble and converted into light by proper choice of standing-wave amplitude and frequency [2]. A burst of light of less than 50 ps duration [3] is emitted in each cycle. If the conditions are appropriate, the bubble can stay stable while it oscillates for hours. The high stability of the flash period suggests that the total mass of the bubble remains constant [2,5].

The experimental analysis has been based on two basic techniques: the measure of the spectral characteristic of the emitted radiation [6] and the measure of the radius of the bubble as a function of time using light-scattered detection. In the former, the scattered intensity is directly related to the radius of the particle by the Mie theory [10], but an independent calibration is needed. The rise-time technique [7] and fitting with a computer simulation were used for this calibration [8]. On the other hand, another type of calibration can be performed using multiple detectors [4], a technique that does not rely on accurate measurements of absolute scattered-light intensity. The purpose of this paper is to explain a new laser-scattering technique based on the Doppler effect [9]. The velocity obtained by this method requires no calibration other than geometrical measurements.

The procedure to measure the bubble interface velocity is based on the fact that when a light ray is scattered by the bubble surface, a small change in frequency (compared with the incident frequency) results. Figure 1 represents a bubble illuminated by a laser beam (only two rays are shown). The Doppler shift is determined by the wavelength of the light, the direction of the scattered light wave, and the velocity.

Both rays in Fig. 1 follow the same output direction (i.e., the same angle  $\phi$  from the forward direction); however, one results from a simple reflection while the other one is a consequence of two refractions. In short, there is a different change in frequency for each of them.

Based on geometrical arguments, the frequency change, in the case of a simple reflection, is given by

$$\Delta \nu_R = \frac{2\|U\|}{\lambda} n_w \cos(\alpha_r), \quad (1)$$

where  $\lambda$  is the light wavelength,  $n_w$  the refraction index, and

$U$  the interface velocity. The following expression gives the frequency change for the second case:

$$\Delta \nu_T = \frac{2\|U\|}{\lambda} [n_w \cos(\alpha_t) - \sqrt{1 - n_w^2 \sin^2(\alpha_t)}]. \quad (2)$$

Looking at the previous equations, both frequency changes are proportional to the absolute value of the velocity (not sign sensitive). The interface velocity can be recovered by measuring the frequency shift. Because the light frequency is on the order of  $10^{14}$  Hz and typical frequency variations are on the order of  $10^8$  Hz, this small relative frequency change cannot be measured directly. The difficulty of measuring small changes in frequency is overcome by means of heterodyne detection [9], the process by which light waves mix over the surface of the light-detector surface. This mixing produces an oscillating signal with a frequency equal to the difference between the frequencies of each wave. In the actual experiment, two laser beams focus on the bubble as shown in Fig. 2. The laser beams, the bubble, and the detector lie on the same plane.

The angle between the detector and one of the beams (K1) is selected in such a way that it corresponds to the critical angle, around  $83^\circ$  for the air-water system. In this case, at first order, the significant ray going to the detector corresponds to the simple reflection. For the second beam (K2), the prior condition does not hold anymore and other rays

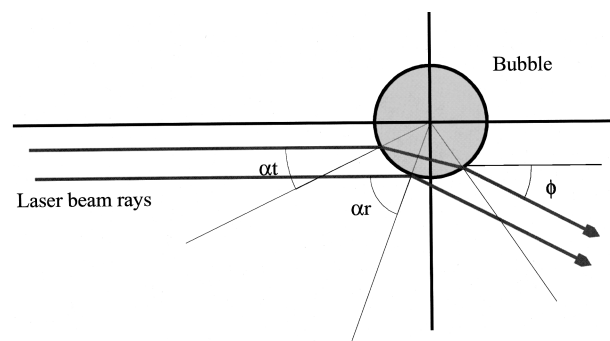


FIG. 1. Laser rays scattered by the bubble. The moving interface causes a small change in the ray frequencies because of the Doppler effect. Even when the magnitudes of the frequency shifts differ, both depend on the absolute value of the interface wall velocity.

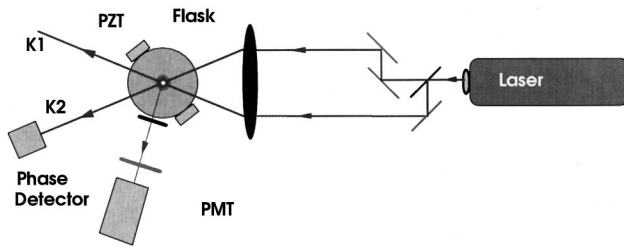


FIG. 2. Experimental setup used in the developed Doppler method to measure the bubble interface velocity. Two parallel laser beams are generated by a beam splitter and mirrors. Both beams are focused over the bubble by a lens.

coming from double refraction and multiple interactions will be present together with the simple reflected ray. The amplitude of the rays decreases as the number of interactions grows. This allows us to consider the interaction of only three rays over the detector. One corresponds to the simple reflection of beam K1 and two rays related to beam K2 (the simple reflection and the double refraction). Due to the ray combination upon the detector, performing a time average over the light period ( $10^{-14}$  s), the signal becomes

$$I = D_c + 2 \sum_{i \neq j} A_i(t) A_j(t) \cos[2\pi(\nu_i - \nu_j)t + \Phi_{ij}],$$

$$i = 1, 2 \quad j = 2, 3, \quad (3)$$

where  $A_i(t)$ , for  $i$  from 1 to 3, is the amplitude of the electric field associated with each ray described before,  $\nu_i$  the frequency shift of each ray, and  $\Phi_{ij}$  the phase difference between the rays  $i$  and  $j$ . The former equation shows a  $D_c$  component (smooth as compared with both light frequency and Doppler oscillations) and three oscillatory terms whose amplitudes depend upon the product of the scattered electric field amplitude of each component.

For the conditions used in the experiments (the angle between beams was around  $30^\circ$  and the detector was at the critical angle from beam K1), we get two high frequencies (HF) that differ less than 20% and one low frequency (LF) equal to this difference. The LF comes from the mixing of the two rays related to the same beam. The phase difference is fixed and, in addition to the velocity, the radius information was also contained in this oscillation. This information was used previously to calculate the radius of the bubble [4] and will be used here to calculate the integration constant to describe the radius.

The Doppler technique was tested using the setup shown in Fig. 2. It was mounted over an optical table. An Argon laser linearly polarized perpendicular to the optical table plane was used to illuminate the bubble. The power of each beam was approximately equal to 7 mW. An air bubble was levitated by a stationary acoustic wave of 29.273 kHz generated in a water-filled spherical flask. The angle between beams was  $30^\circ$ . A silicon p-i-n photodiode with a bandwidth of 125 MHz was used to detect the minimum radius within 20 ns. A TSI photomultiplier with a 150-MHz bandwidth was used to detect the scattered light. The signals were recorded in a HP54111 1 gigasample/s digital oscilloscope.

The collapse part of the cycle is shown in Fig. 3. Oscil-

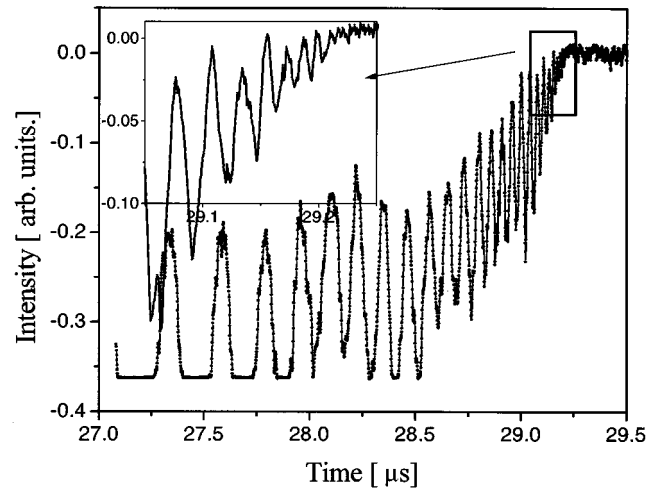


FIG. 3. Experimental data corresponding to a collapse of a sonoluminescent air bubble, close to the upper threshold at  $22^\circ\text{C}$ . The blowup shows the last 200 ns before the collapse. The frequency of the oscillations is proportional to the absolute value of the bubble interface velocity.

lations due to the interference of both beams are present. Moreover, an increase in the frequency is observed as the interface radial velocity increases close to the minimum bubble radius. An enlargement of the last 100 ns is also present.

We used a fast-Fourier-transform filter to compute the  $D_c$  part of the signal. We subtracted the DC part from the original data and, in this way, we isolated the oscillations due to the Doppler frequency change. The time between minimums was used to estimate the frequency and, after substitution into Eqs. (1) and (2), the absolute value of the interface velocity was obtained, as shown in Fig. 4. The time corresponding to each calculated velocity was assumed to be the average between both minimums used in the estimation. Supersonic velocities of 350 m/s were measured with an uncertainty of 20%. The uncertainty is mainly the sum of a sys-

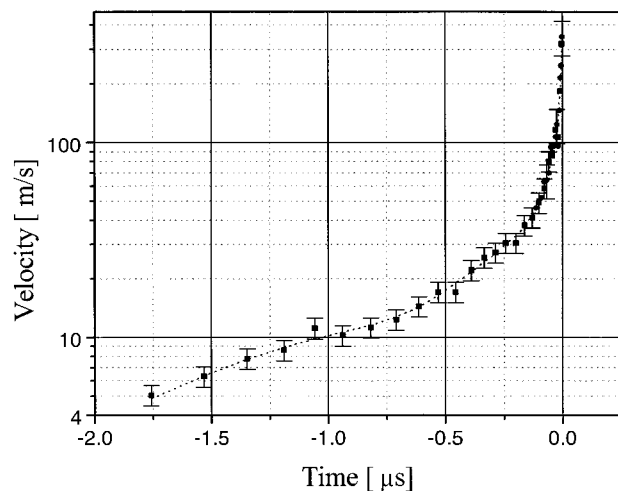


FIG. 4. Interface velocity measurement of a sonoluminescent bubble at  $22^\circ\text{C}$ . Two sets of data are shown. The circles correspond to a higher time-scale resolution in the data acquisition. The uncertainty is between 12 and 20%, as shown by the error bars.

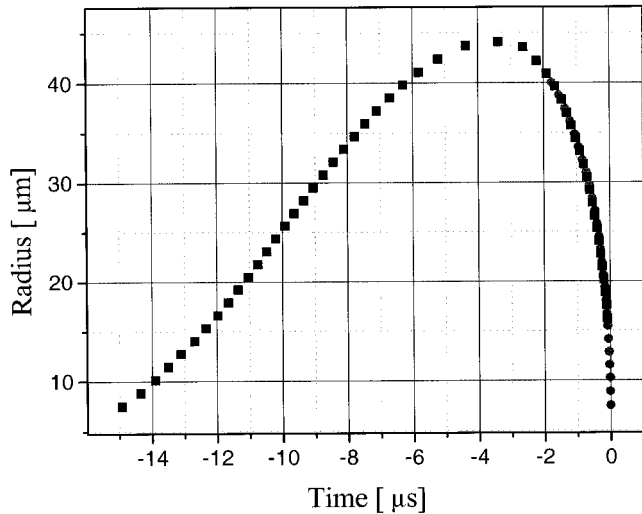


FIG. 5. The radius obtained by integration of the velocity of the same sonoluminescence bubble as a function of time. The integration constant was recovered by contrasting the low-frequency maximums and minimums in the experimental data with the Mie scattering calculation as in [4]. The uncertainty is around  $1.5 \mu\text{m}$ .

tematic error because of the presence of two high frequencies and the uncertainty because the lack of sampling resolution (dominant while velocities larger than  $150 \text{ m/s}$  are present). If the aperture of the detector is increased, the error would also increase.

The radius obtained by a quadrature integration of the velocity (assuming that the radius change between each pair of minimums is constant) and its time variation is presented in Fig. 5. The radius increased about 10 times and attained a maximum radius of  $44 \mu\text{m}$ .

Theoretical Mie scattering calculation was performed by using the differential scattering cross section in [10]. The intensity-radius relationship was transformed in an intensity-time relation according to the radius-time relation obtained for the experimental data. As shown in Fig. 6, excellent agreement with the experimental data was obtained. We also compared the average radius change between maximums with the theoretical result obtained using Eqs. (1)–(3); both agree within less than 1%.

Using the Mie calculation information, each maximum (minimum) in Fig. 6 (solid line) can be related to each maximum (minimum) in Fig. 6 (experimental points). Radius and velocity as functions of time were calculated and are shown in Fig. 7 in a log-log scale. Linear fits corresponding to the last microsecond suggest a critical behavior close to the collapse. This is the first measurement of the key exponent of the bubble free-fall [11]. This number, 0.39, closely agrees with the expected measurement that resulted from the calculations of Barber *et al.* [12]. For bubble radius ( $R$ ) smaller than half the maximum radius ( $R_m$ ), they obtained

$$\dot{R}R^{3/2} \approx -(2P_0/3\rho)^{1/2}R_m^{3/2} = Cte. \quad (4)$$

From Fig. 7,  $R \propto t^\alpha$  then,  $\dot{R} \propto t^{1-\alpha}$ ; therefore, from Eq. (4),  $\alpha$  has to be 0.4.

The small distance between the experimental points and the line suggests that the systematic error due to the presence

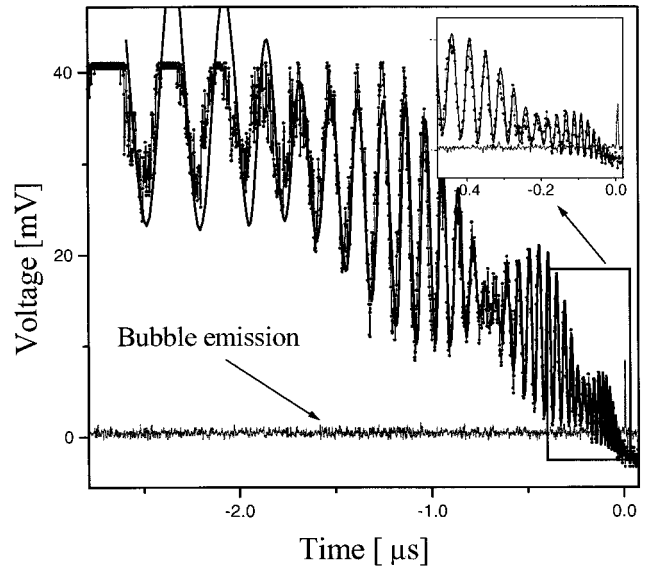


FIG. 6. Comparison between the experimental Doppler oscillations (dots) and a Mie scattering simulation (originally calculated as an intensity-radius relationship) in the same conditions. The agreement between both curves is excellent. The sonoluminescence light peak (lighter line) can be also observed.

of two frequencies has been reduced to less than 10%. The collapse time was assumed to be the time corresponding to the maximum in the sonoluminescence emission detected by another photomultiplier tube.

In conclusion, a technique to measure the bubble interface velocity and bubble radius was presented. Velocity can be obtained directly without calibration, i.e., the detection method is independent of the absolute scattered intensity. Experimental results, which agree with theoretical simulation

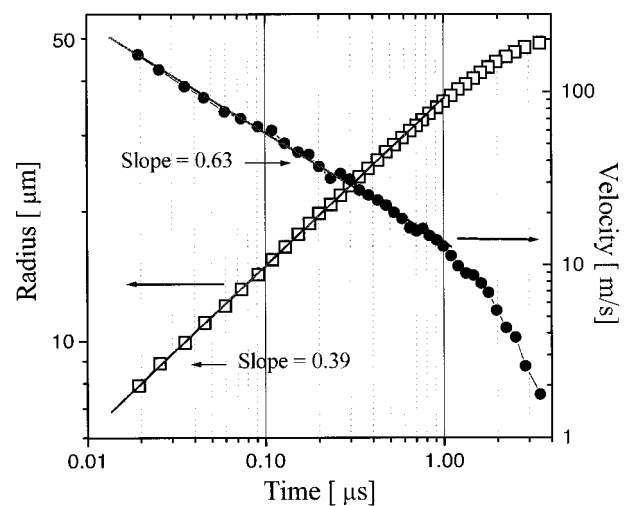


FIG. 7. Experimental radius and velocity in the last  $\mu\text{s}$  of a sonoluminescent bubble cycle, previous to the minimum radius. The slope of the linear fit agrees very well with the theoretical calculation in [12]. The integration constant was obtained by a direct comparison between the experimental data and the Mie theoretical calculation (Fig. 6).

of the scattered-light-expected a relationship between velocity and frequency variation [Eqs. (1)–(3)], also compared well with computational simulation. Moreover, velocities and radius compared well with their respective measurements obtained in [4].

Supersonic velocities of 350 m/s were measured within 20%, occurring at  $10 \pm 10$  ns to the minimum radius. This condition suggests the presence of shock waves in the gas.

Critical phenomenon behavior was observed close to the light emission, behavior that supports the existence of a self-similar solution in this region. Although the maximum measured velocity was 350 m/s, based on the tendency of the experimental data, higher velocities were expected.

We thank Richard Lahey Jr., Robert Block, Pankaj Das, and Claire Ryan for their contributions.

- 
- [1] N. Marinesco and J. Trillat, *C. R. Hebd. Seances Acad. Sci.* **196**, 858 (1933).
- [2] D. F. Gaitan *et al.*, *J. Acoust. Soc. Am.* **91**, 3166 (1992).
- [3] B. P. Barber and S. J. Putterman, *Nature (London)* **352**, 318 (1991); R. Hiller, S. J. Putterman, and B. P. Barber, *Phys. Rev. Lett.* **69**, 1182 (1992); B. P. Barber *et al.*, *ibid.* **72**, 1380 (1994).
- [4] W. J. Lentz, A. A. Atchley, and D. F. Gaitan, *Appl. Opt.* **34**, 2648 (1995).
- [5] M. P. Brenner *et al.*, *Phys. Rev. Lett.* **76**, 1158 (1995).
- [6] R. Hiller *et al.*, *Science* **266**, 248 (1994); R. A. Hiller and S. J. Putterman, *Phys. Rev. Lett.* **75**, 3549 (1995).
- [7] R. G. Holt and L. A. Crum, *Appl. Opt.* **29**, 4182 (1990).
- [8] B. P. Barber and S. J. Putterman, *Phys. Rev. Lett.* **69**, 3839 (1992); R. Lofstedt *et al.*, *Phys. Rev. E* **51**, 4400 (1995).
- [9] F. Durst, A. Melling, and J. Whitelaw, *Principles and Practice of Laser Doppler Anemometry*, 2nd ed. (Academic, New York, 1981).
- [10] P. W. Barber and S. C. Hill, *Light Scattering by Particles: Computational Methods* (World Scientific, Singapore, 1990).
- [11] Suggested by the reviewer.
- [12] B. P. Barber *et al.*, *Phys. Rep.* **281**, 65 (1997).